World Academy of Science, Engineering and Technology
International Journal of Mechanical and Materials Engineering
Vol:16, No:5, 2022

Literature Review on Metallurgical Properties of Ti/Al Weld Joint Using Laser Beam Welding

K. Kalaiselvan, Naresh Subramania Warrier, S. Elavarasi

***Abstract*—**Several situations arise in industrial practice which calls for joining of dissimilar metals. With increasing demand in the application requirements, dissimilar metal joining becomes inevitable in modern engineering industries. The metals employed are the structure for effective and utilization of the special properties of each metal. The purpose of this paper is to present the research and development status of titanium (Ti) and aluminium (Al) dissimilar alloys weldment by the researchers worldwide. The detailed analysis of problems faced during welding of dissimilar metal joint for Ti/Al metal combinations are discussed. Microstructural variations in heat affected zone (HAZ), fusion zone (FZ), Intermetallic compound (IMC) layer and surface fracture of weldments are analysed. Additionally, mechanical property variations and microstructural feature have been studied by the researchers. The paper provides a detailed literature review of Ti/Al dissimilar metal joint microchemistry and property variation across the weldment.

***Keywords*—**Laser beam welding, titanium, aluminium, metallurgical properties.

I. Introduction

WELDING of dissimilar metal depends on the metallurgical compatibility. Several metallurgical and thermophysical variations can occur due to cooling of welding cycle and phase transition during solidification [1]. The formation of the joint affects the quality of assembly. Metallurgical compatibility and poor chemical affinity can result in brittle interface. This needs the improvement of weldability of dissimilar metal weld through understanding and control of the IMC layer. Many researchers conducted mechanical and chemical analyses on several titanium (Ti) and aluminium (Al) IMC to check their ductility and strength [2]. Additionally, diffusion welding of Ti and Al multi laminated combination formed $TiAl_3$ depends upon the high temperature from 660 to 680 ºC [3].

Ti and Al metal combinations are studied by using Friction Stir Welding (FSW). During welding Al side was plunged by the tool pin. The particles of Ti in the Al matrix elongated less than the surrounding of Al leading to the formation of cavities in the nugget zone during the stirring action [4]. Some difficulties were highlighted during FSW dissimilar metal butt weld joint because of their tendency to crack and to form grooves due to the high speed tool rotation [5]. Welding processes are mostly exploited in traditional fabrication and innovative products. Metal joining is very popular in modern production industries. Solid state and fusion welding process is used in different products and metals [6]. In fusion welding techniques, the laser beam has gained a prominent position as an autogenous melting source for metal joining [7]. It melts the surrounding material and high energy vaporizes a cavity using thick structural steel plates [8]. Compared with other fusion techniques, laser beam welding (LBW) can be considered as a desirable thermal source for controlling interfacial reaction layer [9].

Many researchers concentrated LBW with different properties. During welding the laser light irradiates the Al surface melts and solid surface of Ti wets. Disadvantages of interfacial reaction reduce the mechanical properties and initiation of cracks of weldment [10]. Laser beam focusing on Al side is a challenging one and weld seam quality is affected negatively [11]. In fibre laser it produced high performance welding using Ti alone [12]. High speed full penetration fibre laser welding of Ti and Al weld joint was investigated [13]. The formation of IMC layer thickness can reduce using fibre laser [14]. Without chamfering and filler metals laser beam can focus on Ti side at a close distance from the centre line of the weldment which is called as offset welding [15]. Using optical and electron microscopes, the effects of the welding conditions on the IMC layer were studied. The solidified interface formed from the Ti HAZ were studied as welded and post weld heat treatments (PWHT) [16].

The same approach was used for magnesium and steel dissimilar welding [17]. Laser welding with Al and steel has proved to be viable [18]. Laser arc hybrid welding of high strength steel and Al alloy joint with brass filler demonstrated that the braze weld joint fabricated without Cu-Zn interlayer fractured at the Al-Fe IMC [19]. The main motive of this review paper is to know the research and development of titanium (Ti) and aluminium (Al) dissimilar metal weld joint using LBW. The detailed literature review with reference to metallurgical properties has been discussed in this paper. Characterization and analysis work of Ti/Al dissimilar weldment by different authors have been discussed.

II. Metallurgical Properties

Laser welding-brazing of Ti6Al4V and 5056Al was conducted using AlSi12 filler metal. The metallurgical characteristics of weld joints were analysed by scanning electron microscope (SEM), energy dispersive spectroscopy

Dr. K. Kalaiselvan, Principal, is with Kerala Technological University Affiliated Engineering College, Calicut, Kerala, India – 673601 (phone: 8891491686, e-mail: kalaiesanai@gmail.com).

Dr. Naresh Subramania Warrier, Chief Executive Officer, is with the Kerala Technological University Affiliated Engineering College, Calicut, Kerala, India – 673601 (phone: 8592020104, e-mail: naresh.warrier@gmail.com).

S. Elavarasi is with the Department of Civil Engineering, Anna University Affliated Engineering College, Trichy, Tamilnadu, India-620007 (e-mail: elavarasiselvaraj2000@gmail.com).

(EDS) and optical microscopy [20]. The results showed that the joint is divided into a welding part on the aluminium (Al) side and brazing part on the titanium (Ti) side. An IMC layer formed at the brazing interface between mixed seam metal and titanium. The IMC layer at the interfacial top includes an acicular TiAlSi intermetallic layer and a continuous Ti/Al IMC near titanium alloy. The IMC layer at the interfacial bottom is thin and different from that at the top.

The fibre laser welding of thin AA6061 and Ti6Al4V was performed by focusing the laser beam on the Ti alloy side. The effect on the microstructure and formation of interfacial IMC layer of the dissimilar butt joint were discussed [21]. Fig. 1 (a) shows the cross sections of the weldment. The Ti is the left side while the Al is the right one. Both sides show a FZ and a HAZ. The fusion of the Ti was due to the classic keyhole welding mode. The heat transfer from Ti to Al produced the continuity of the FZs. Fig. 1 (b) shows the magnification of the bimetallic interface. The IMC layer was made of Ti_3Al and $TiAl_3$ compounds.

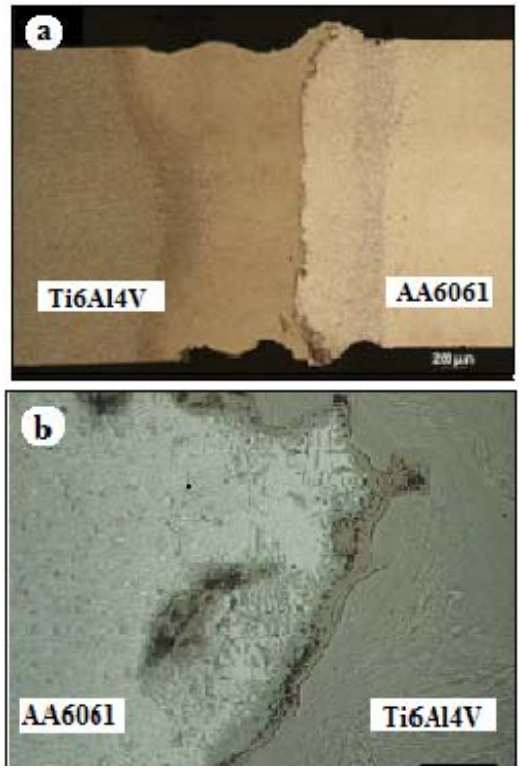

Fig. 1 (a) Weldment cross section and (b) Magnification of the bimetallic interface

Joining mechanism of Ti/Al dissimilar alloy was investigated using laser welding brazing process with automated wire feed [22]. The microstructures of fusion welding and brazing were analysed in details by transmission electron microscope (TEM). It was found that microstructures of FZ consist of α-Al grains and ternary near-eutectic structure with α-Al, Si and Mg_2Si. Interfacial reaction layers of brazing joint were composed of α-Ti, nano-size granular Ti7Al5Si12 and serration-shaped $TiAl_3$. Structure in IMC phase $TiAl_3$ was found when the thickness of the reaction layer was approximately less than 1 μm.

Joining of 5A06Al and Ti6Al4V alloys with a good appearance of weldment was achieved by laser welding using AlSi12 filler wire [23]. The interfacial microstructure of the joints with a melting mode is much more complex as shown in Fig. 2. Granular compounds, filamentous structure and solid-state phase changes reaction layer appear at the interface. According to the results obtained from the x-ray diffractometer (XRD) and EDS study, interfacial microstructure is divided into five layers such as solid-state phase changes reaction layer with Ti_3Al and precipitation Ti_5Si_3 (I), eutectic reaction layer with TiAl and Ti_5Si_3 (II), hypoeutectic reaction layer of Ti_5Si_3 and primary TiAl (III), hypereutectic reaction layer of primary Ti_5Si_3 and TiAl (IV) and discontinuous reaction layer with Ti (Al, $Si)_3$ (V). Granular compounds Ti_5Si_3 are surrounded by the IMC phase TiAl in the hypereutectic reaction layer. The serration shaped reaction layer still consists of the IMC Ti (Al, $Si)_3$.

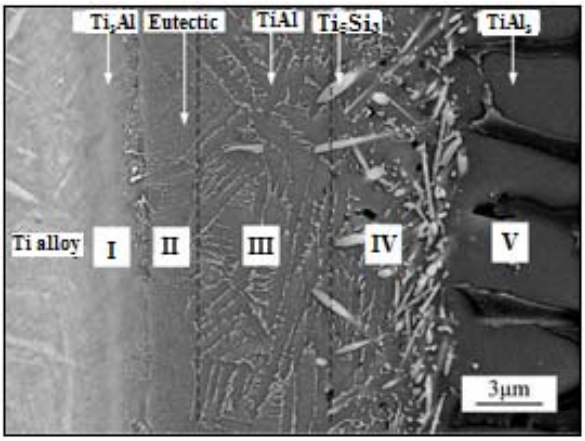

Fig. 2 Interfacial microstructure of Ti/Al alloys joint

Dissimilar welding of Ti and Al metals was carried out under the Al-Ti and Ti-Al combinations at various welding speeds using single mode fibre laser having high power density. It was confirmed that the high welding speed of 50 m/min could reduce the formation of brittle IMC such as Al_3Ti and Al_2Ti. Mainly, Al_3Ti IMCs were generated in Al-Ti and Al_2Ti was produced in Ti-Al. A needle-shaped martensitic Ti phase was provided under Al-Ti condition at 50 m/min welding speed [24]. On the other hand, martensitic Ti phase was not generated on the Ti-rich side of a FZ and small size dendritic phases and island type phases of IMC formed from Ti phase. Combination of Ti and Al sheet metals produced strong weldment using single mode fibre laser with high speeds.

The laser welding–brazing of Ti6Al4V and 5A06 alloys with a 1.5 mm thickness in a butt configuration was carried out by laser beam focusing on Al alloy side without a filler metal [25]. The cross section of the weld joint is shown in Fig. 3 (a). It is mainly divided into three stages such as Ti zone, Al FZ and Al zone. During welding-brazing Al liquid was spread

over the Ti plate. Fig. 3 (b) shows the local graph of cross-section. Titanium element was diffused in the in the interface and to form new Ti rich crystal. Al liquid spreading length is maximum over the Ti plate. Fig. 3 (c) shows the microstructure of the cross section located at the C region in Fig. 3 (b). Ti alloy microstructure consisted of α and β phases in which α phase was surrounded by the β phase [26]. IMC layer was formed in between Ti ally and the FZ. Few Ti elements infiltrated into the FZ to form the laminated Ti-rich compounds. Fig. 3 (d) shows the microstructure of the cross section located at the A region in Fig. 3 (b).

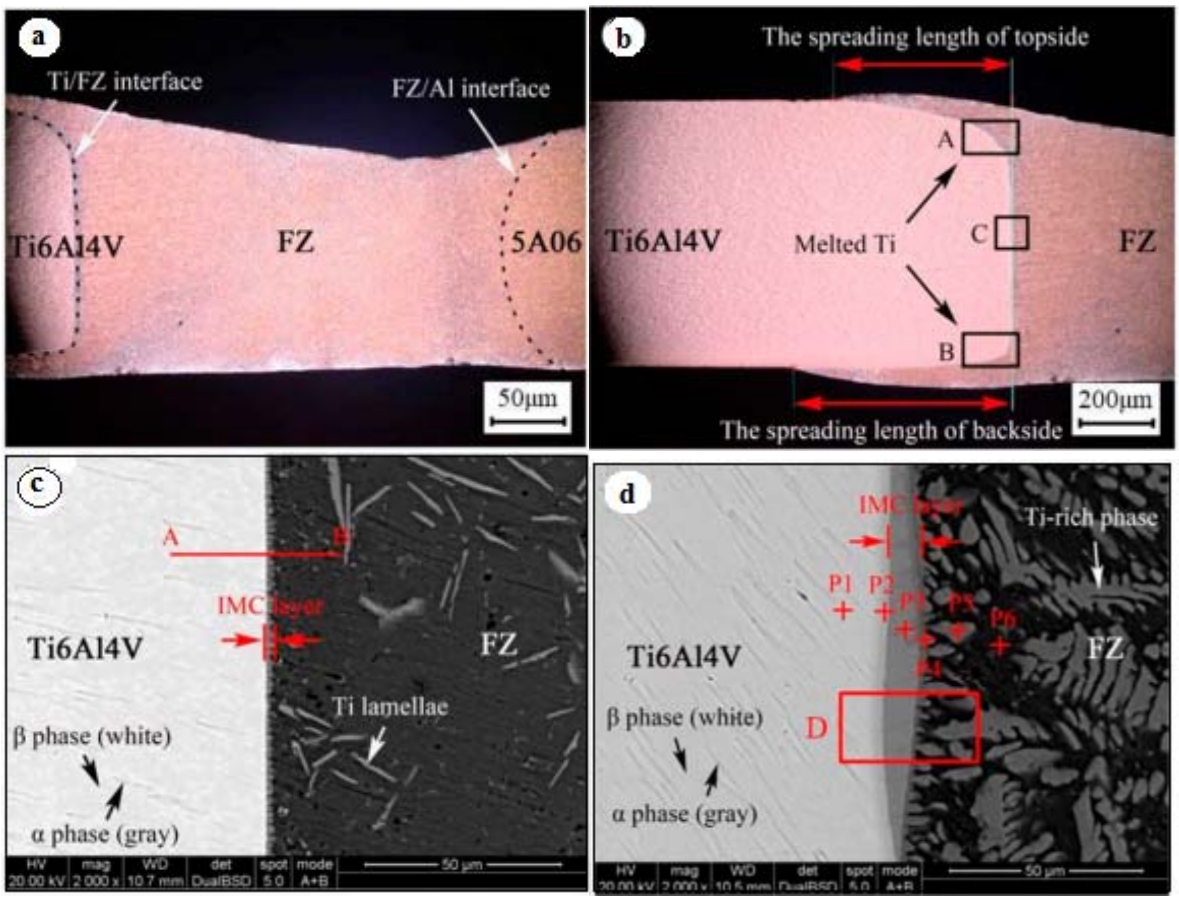

Fig. 3 Cross section of the joint: (a) macro cross section, (b) local graph of cross section, (c) SEM image of the C region and (d) SEM image of the A region

Dissimilar LBW of AA6056 and Ti6Al4V alloy are produced by inserting Ti-sheet into the profiled Al-sheet and melting AA6056 alone. Uneven microstructure and localized plastic deformation due to strength mismatch were investigated [27]. Cracks were parallel and perpendicular to the weld for fatigue crack propagation and fracture toughness at room temperature. Also, brittle intermetallic $TiAl_3$ had been formed at the interface. Crack propagation is faster than that of HAZ and FZ. A feature in crack propagation is the steeper slope occurred after initial stabilization. Striations are observed from the AA6056-T6 base metals over the entire fatigue crack propagation region shown in Figs. 4 (a) and (b). Dimples and striations are observed on FZ cracks as shown in Figs. 4 (c) and (d). In FZ, cracks are parallel to the weldment. Crack length is increased and formed striations. All the changes occurred in the fracture mode but not in the base metal of AA6056. It is observed that due to the presence of dimple, the strength is exceeded. The slope of fatigue propagation increased depending upon the striation mode.

The possibility of direct high speed Yb:YAG laser welding of AA5754 to Ti6Al4V alloys keyhole mode has been explored. In order to understand the influence of contact interface on the tensile strength of the weldment, the fracture surface of the weld joint obtained after tensile test was studied by SEM [28]. Under all operational conditions, the fracture involved contact interface situated between Al and Ti-rich melted zones. It was found that morphologies of contact interface result in the mode of fracture illustrated by SEM topography structure as shown in Fig. 5. The sample having thin contact interface present fracture surface composed by zone of Al and containing various proportions between Ti and Al. The zones containing both Ti and Al present cleavage fracture mode and contain mixtures of different intermetallics, where TiAl phase dominates. Crack initiates in a thin contact interface surface due to Ti_3Al situated at titanium interface side and propagate near Al-rich zone. High tensile strength of

such weld joint can be attributed to higher mechanical stability and more ductile behaviour of Al zone comparing to brittle intermetallic zones.

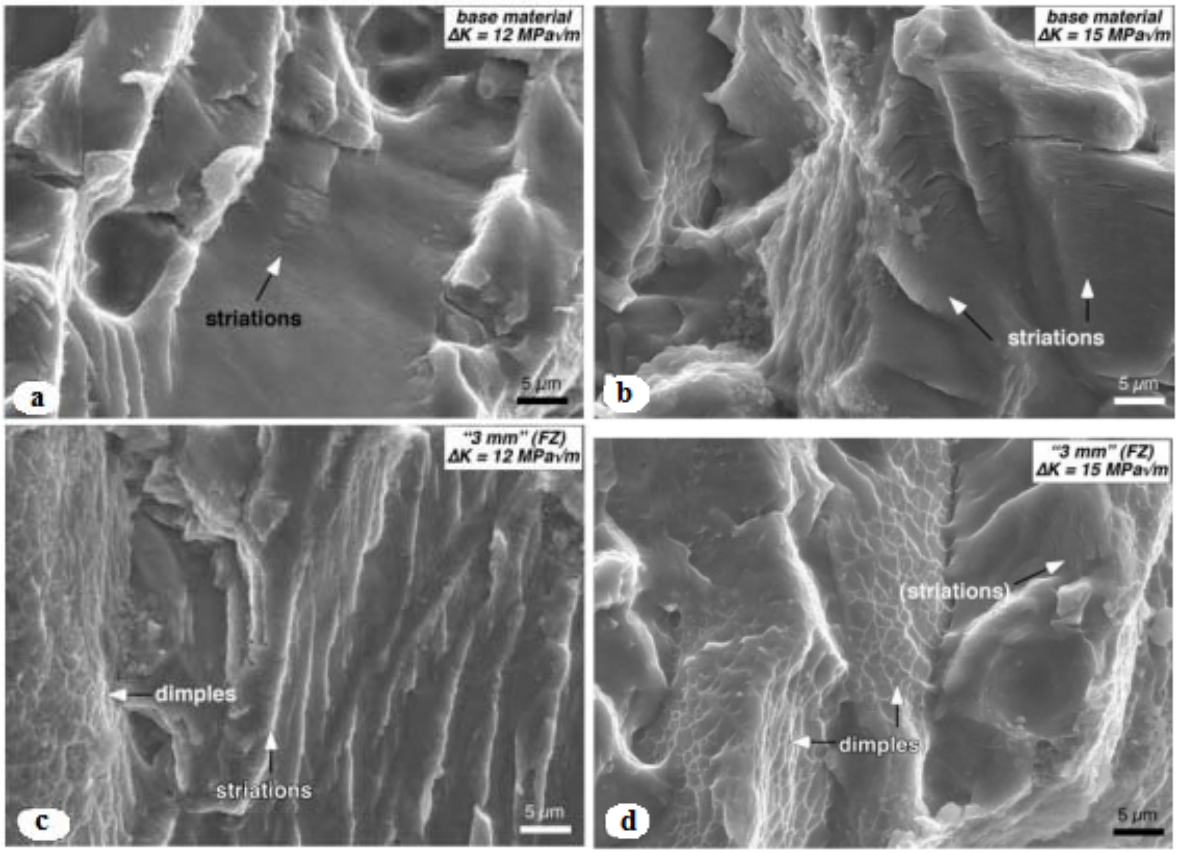

Fig. 4 (a) Fatigue crack propagation in AA6056, (b) Fatigue crack propagation in T6, (c) and (d) FZ crack

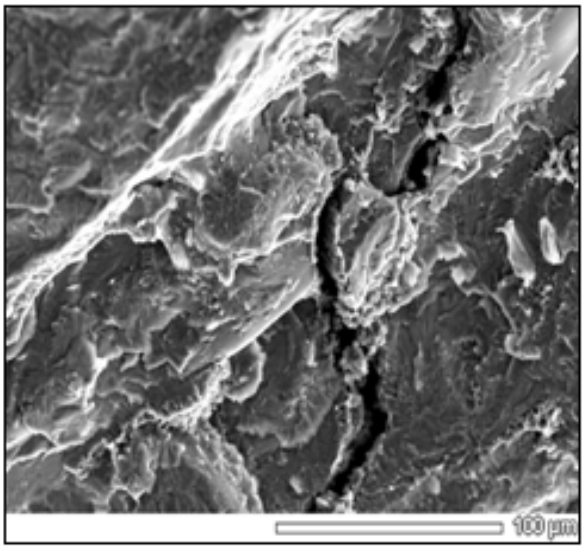

Fig. 5 SEM image if fracture surface

5A06 and Ti6Al4V combinations are joined by using CO_2 spot laser welding brazing with the filler metal of Al-12Si. During welding Si diffusion behaviour has a significant effect on the formation of IMC [29]. To analyse the Si diffusion behaviour, a model for the prediction of the chemical potential for alloy was established. According to the results of the influence of the element content and temperature in TiAlSi system on Si chemical potential, the diffusion of Si element was analysed for Ti dissolution and melting mode, which presents a better agreement with the experimental data.

The interfacial characteristics of dissimilar Ti6Al4V/ AA6060 weld joint were produced by pulsed Nd:YAG LBW [30]. The interface interaction relationship of the weld joint is analysed by SEM as shown in Fig. 6. The potential phases of TiAl and $TiAl_3$ were observed near the Ti/Al interface. The propagation path of phase change in the Ti/Al interface can be explained by mismatch in thermophysical properties and by thermodynamic factor. As the Ti6Al4V has much higher fusion temperature than AA6060, the volume of melted Al was much larger than the volume of melted Ti. Due to the high solidification rates proper to laser welding, the main solidification process was the local equilibrium at solid–liquid interface and the convective mixture between melted materials is poor. Based on the analysis, it can be indicated that the rapid rate with respect to cooling or solidification rate seriously affected the crack initiation. It should be noticed that the time available for the residual liquid to refill and heal the initiated cracks may be mitigated by high cooling rates.

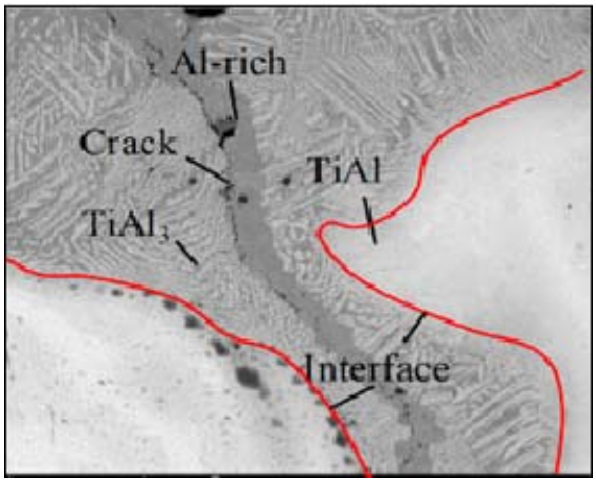

Fig. 6 Phase distribution in the Ti/Al interface

The phase relations in the titanium (Ti), aluminium (Al) and silicon (Si) system were undertaken by differential thermal analysis, metallography, X-ray diffraction and microprobe analysis [31]. The measurements were combined with the investigation of this alloy composition in the TiAlSi system. The mixed results allowed the construction of a solidus projection, a melting diagram of solidus and liquidus, partial isothermal sections at 1270 °C and 1250 °C, three isopleths with a constant percentage of one another components and a reaction scheme.

Fibre laser-cold metal transfer arc hybrid welding was developed to join AA6061 to Ti6Al4V alloys in butt configuration. The optimal range of heat input for the accepted joint was obtained, which is 83-98 $J \cdot mm^{-1}$. Approximate laser power of 2.5 kW, both the volume of liquid metal generated by heat input and the depth of outward and upward flow were sufficient to fully cover the Ti sheet. This causes an accepted joint without root defect [32].

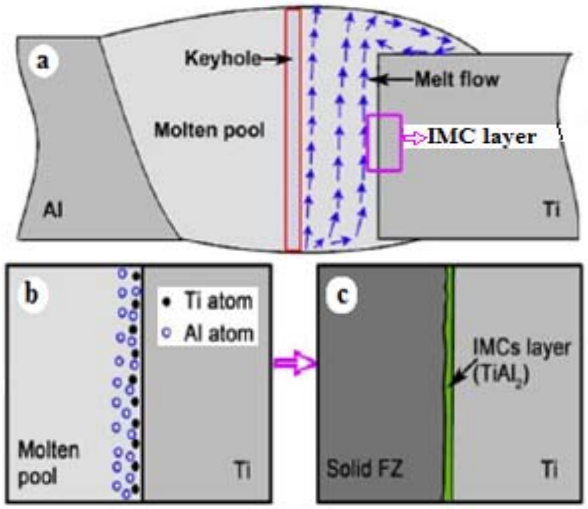

Fig. 7 IMC layer growth, (a) Appropriate laser power, (b) IMC layer formation and (c) IMC layer

A sufficient interface reaction was achieved due to enough heat input, resulting in an IMC layer with appropriate thickness as shown in Fig. 7 (a). At this stage, the formation process of IMC layer is illustrated in Fig. 7 (b). Some Ti atoms first dissolve into molten pool during the heating stage. Subsequently, dissolved Ti atoms react with Al atoms to form $TiAl_2$ along a liquid/solid interface as shown in Fig. 7 (c). The formation of $TiAl_3$ is suppressed, which would be attributed to fast cooling rate of hybrid welding [33].

The corrosion behaviour of the Nd: YAG laser and gas metal arc (GMA) welds of the AA6061-T6 alloy were reported in [34]. The surface morphology observation and composition analysis were investigated by SEM with energy dispersive X-Ray (EDX) spectroscopy. An increase in the precipitate phase was observed in the weld fusion zone (WFZ). The WFZ suffers more pitting and cracks. It is suggested that the increased precipitate phase increased the galvanic corrosion couples and resulted in aggravation of pitting and crack in the WFZ.

The dissimilar joining of T40 with A5754 alloys were welded by using LBW [35]. After welding the metallurgical properties are observed. The SEM-EDS analysis of interfacial layers indicates that a serrate-shape $TiAl_3$ intermetallic (IM) mostly forms between solid Ti and liquid Al, with thickness ranging between 0.5 and 2.4 μm, which are constantly increasing with the volumetric energy as shown in Figs. 8 (a) and (b). Such layers are thicker near the external edge of welds, where the laser-induced temperature profile was higher and tend to decrease toward the internal part of the weld.

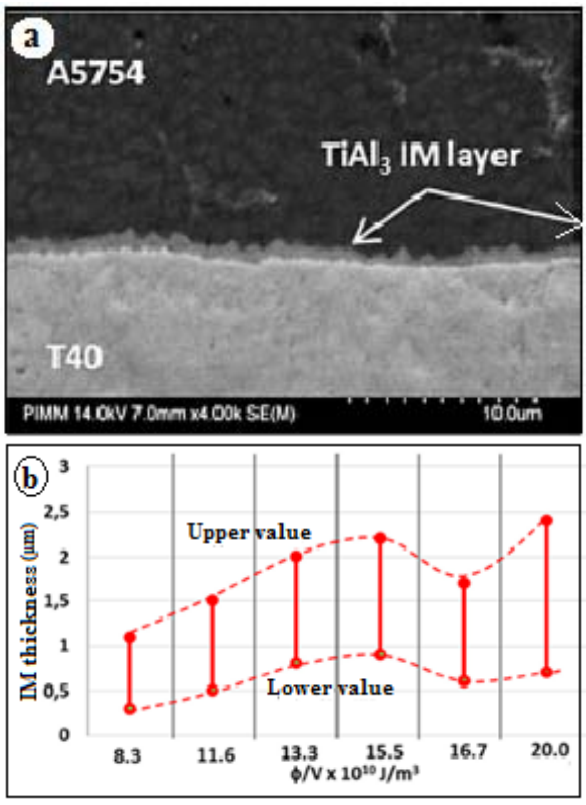

Fig. 8 SEM-EDS analysis of interfacial layers: (a) IM thickness and (b) IM thickness versus volumetric energy

For IM average thickness below 0.5 μm, the IM becomes strongly heterogeneous and does not involve the whole interface. The resulting effect is that local thermal stresses generated during the phase growth and subsequent cooling have been sufficiently high to provoke interface de-bonding. The resulting effect is that molten aluminium is debonded from Ti, even if Ti has been correctly wetted. Consequently, a minimum interfacial temperature is necessary to ensure an optimal and uniform bonding between Ti and Al.

Dissimilar welding of Ti and Al using single mode fibre laser with high welding speed and microstructural characteristics of the interlayer in the Ti and Al weldment was observed [36]. Full penetration welding was tried. The intermetallic phases and areas of the welded zones are observed by SEM and analysed by using XRD. The results suggest a formation possibility of a strong Ti and Al dissimilar weld with IMC reduced by a single mode fibre laser under the condition of high welding speed.

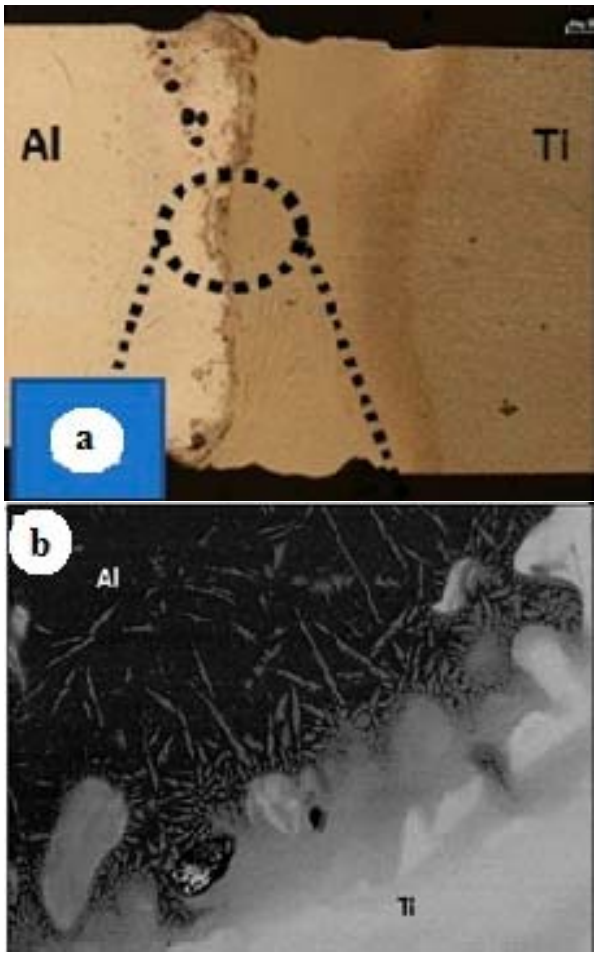

Fig. 9 (a) Weldment cross section and (b) IMC layer

Laser beam on the weldability of Ti6Al4V to 6061 alloys dissimilar butt weld was presented. The data coming from the metallurgical characterization of the weld were analysed [37]. Fig. 9 (a) shows the cross section of the weld joint. For the joint, the laser beam produced key hole which was focused on the Ti side. The FZ of Al was generated through the Ti-Al interface by heat. Therefore, the weld joint exhibited FZ by Al side and Ti side which separated by IMC layer. Fig. 9 (b) shows a SEM micrograph of the IMC layer in the highlighted circle. For dissimilar Ti and Al alloys joint, the composition of IMC layer is not uniform, varying from Ti_3Al to Al_3Ti as the distance from A side FZ increases. The hardness of the weldment increases from Al_3Ti to Al_3Al and other mechanical properties are not even along the thickness.

The phase equilibrium in the TiAlSi system is observed in the temperature range 700–1000 °C using ternary diffusion couple experiment with pure Ti and AlSi eutectic alloy [38]. Some binary and ternary IMCs have been observed. The IM such as $TiAl_2$, Ti_9Al_{23}, Ti_3Al and TiAl formed as solid layers. The IM Ti_5Si_4 and Ti_5Si_3 are found as two-phase layers associated with $TiAl_3$. Two ternary IMCs τ_1 and τ_2 with compositions close to $Ti_3Al_2Si_5$ and Ti_3AlSi_5 are noted. Also, the microstructure of binary and ternary phases has been reported.

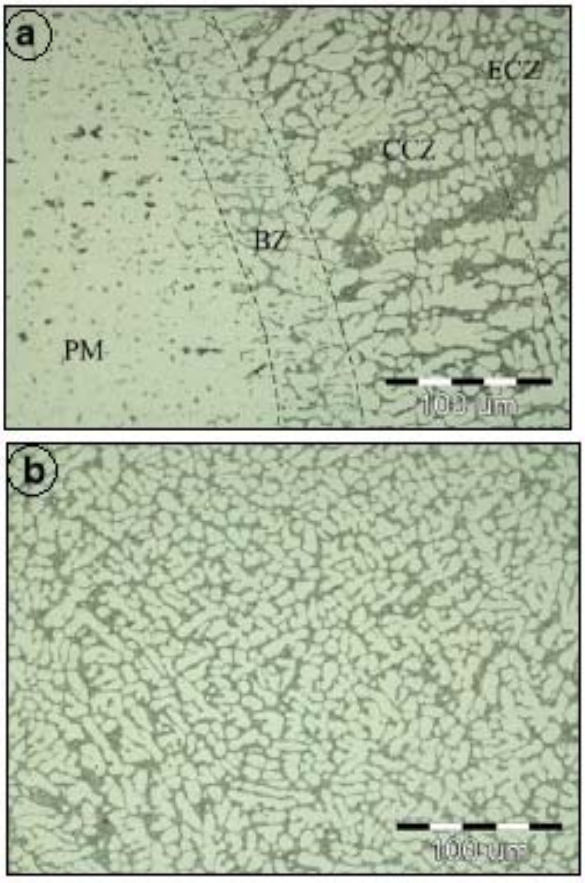

Fig. 10 Microstructures of the weld joint, (a) Microstructures of the FZ near Al matrix and (b) Equiaxed crystal structure in FZ

Ti/Al dissimilar alloy joint was performed by a rectangular spot laser welding-brazing method. The microstructural properties of the weld joints were characterized. During the welding-brazing process, fusion welded joint is formed by the melted Al alloy and filler wire [39]. The influences of heat

input on the microstructure of the fusion welding joint are not significant. Fig. 10 shows the microstructure of fusion welded joint. As shown in Fig. 10 (a), there were four different zones such as parent metal (PM), bond zone (BZ), columnar crystal zone (CCZ) and equiaxed crystal zone (ECZ). Fine hypoeutectic microstructure was formed at BZ. The diffusion of Si element from molten pool to BZ leads to the formation of the hypoeutectic structure. The microstructures in CCZ and ECZ are similar to that in BZ as partial melting Al alloy matrix mixed with the completely melting filler wire. The CCZ contains coarse columnar α-Al solid grains and eutectic structures. The coarse columnar structure is nearly vertical to the bond line, which is induced by higher cooling rate and obvious direction of thermal conduction. Equiaxed α-Al grains and eutectic structures compose the ECZ, as shown in Fig. 10 (b).

Commercially pure Ti and pure Al were subjected to traditional methods of welding. These two metals lead to the formation of brittle IMCs that compromise the quality of the joint [40]. The problem stems from the extreme difference in the welding temperature of the two metals and the different thermal expansion and conductibility coefficient values are higher for Al. These two metals are permanently joined by LBW. Microstructural characterization by SEM and metallographic techniques were adopted to highlight the transformation of these metals.

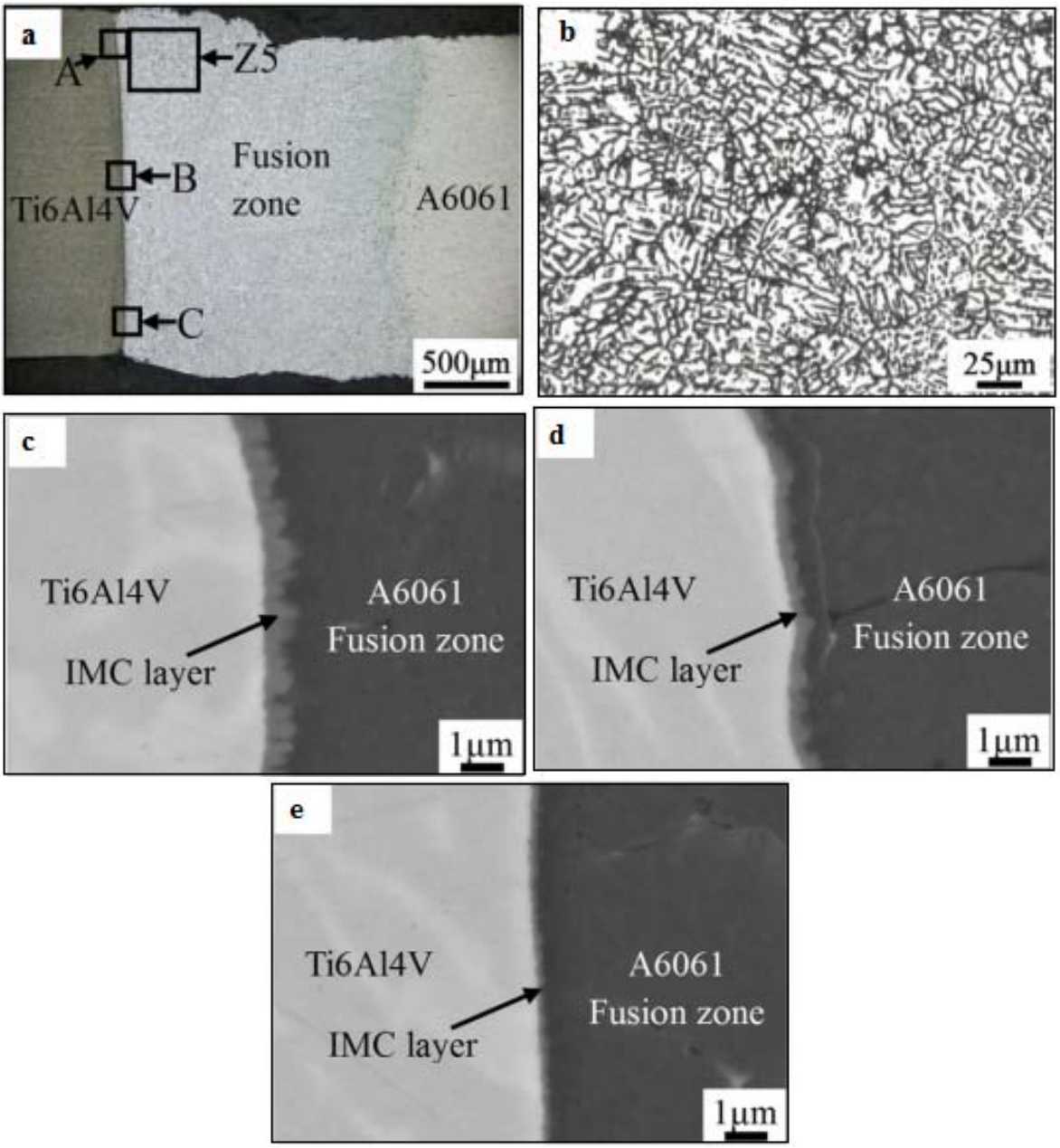

Fig. 11 (a) Cross section of the joint, (b) Z5- Zone microstructure, (c) Interfacial microstructure of zone A, (d) Interfacial microstructure of zone B and (e) Interfacial microstructure of zone C

Cross section appearances of Ti6Al4V/A6061 laser welded joint with laser offset of 0.9 mm is shown in Fig. 11 (a) [41]. It is clear that titanium is not melted, while the melted aluminum wets titanium surface at the interface, so that brazing joints are produced. Fig. 11 (b) shows 5-zone microstructure of the weldment near by the interface. The dendrite arm spacing (DAS) are present in the FZ. The SEM backscattered electron images of three zones such as zone A, B and C are shown in Figs. 10 (c)-(e) for the joint. The interfacial IMC layer is a discontinuous serrate-shape. Obviously, the thickness of the IMC layer tends to decrease from top zone (zone A), through middle zone (zone B) to bottom zone (zone C) of the joint. The IMC layer thickness is about 0.8 mm in the top zone and 0.2 mm in the bottom zone. The average thickness of IMC layer in zone A, B and C is 0.48 mm.

Laser assisted joining of AA5754 to T40 alloys with use of AlSi filler wires was carried out. Continuous experimental design method was applied to study the influence of operational parameters on the properties of the joints [42]. The morphology study was focused on the dissimilar interface. It was found that interface morphologies might coexist in a single sample because of a difference in local thermal history. Fig. 12 shows the morphology of interface composed by well-developed columnar structure. The thickness of the interface was comprised between 13 and 25 µm.

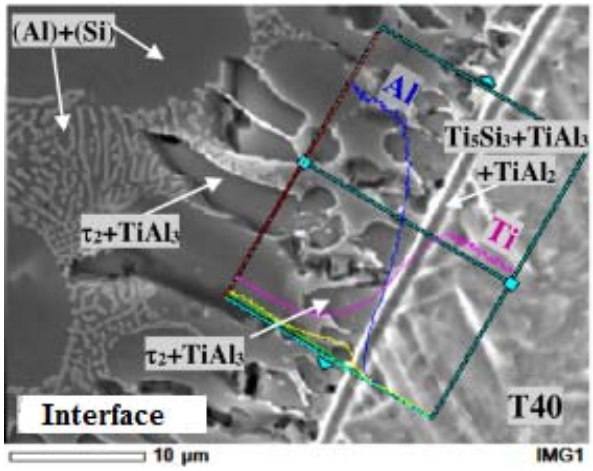

Fig. 12 Interface morphology

The global view of fractured surface on titanium side is shown in Fig. 13 (a). It shows Al-Si-rich zone and Ti-rich zones. The tooth-like character of the interface between these two zones corresponds to the periodical arrival of melted filler wire at the bottom of the groove. In Al-Si rich zone, transgranular fracture mode was observed and clearly shown in Fig. 13 (b).

The fracture took place in the proximity of titanium interface, as the concentration of Si was systematically superior to that of filler wire. Visible Ti-rich zone is in fact the surface of titanium groove that suffered from weak adherence of filler material. In this zone, brazing was inefficient due to insufficient energy supply. These zones were generally situated at the middle or bottom of the weldment.

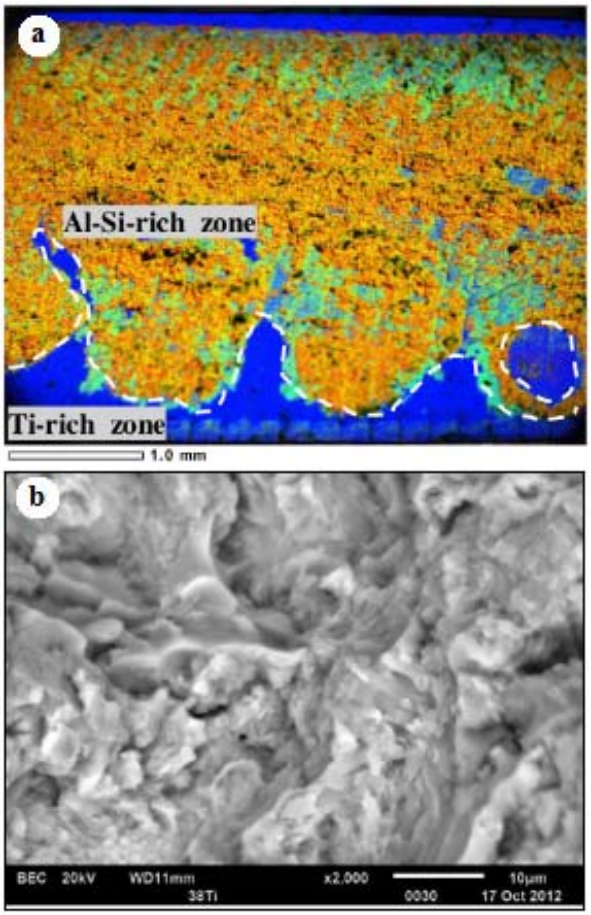

Fig. 13 Fracture surface (a) X-map of global view and (b) Zoom on fracture surface in Al-Si rich zone

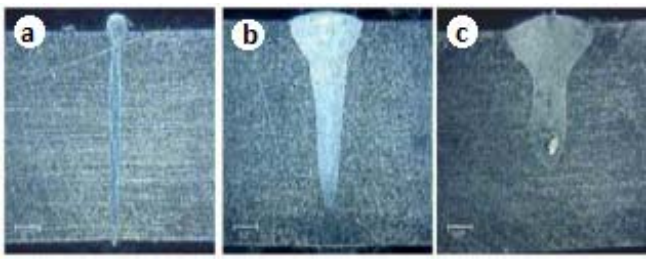

Fig. 14 Cross sections of bead on plate welds for single mode and multimode

In a single mode, all power concentrated on one particular point and produced taper shape. Due to high intensity during welding, small gap is produced in the joint, [43]. The multimode laser beam more equally distributes its intensity across the weld resulting in more stable welding conditions. Fig. 14 shows cross sections of bead on plate welds for single mode and multimode lasers in 0.06" thickness utilizing (a) Single Mode Laser at 500 W and 300 ipm with a 30 micron spot size; (b) Multi Mode Laser at 700W and 100 ipm with a 150 micron spot size; (c) Multi Mode Laser at 1 kW and 80 ipm with a 250 micron spot size. There are some cases where single mode lasers can be implemented effectively in welding

applications with high-speed welding. Using lower laser power, it is possible to weld very close joints. But using multi-mode lasers achieve a good penetration.

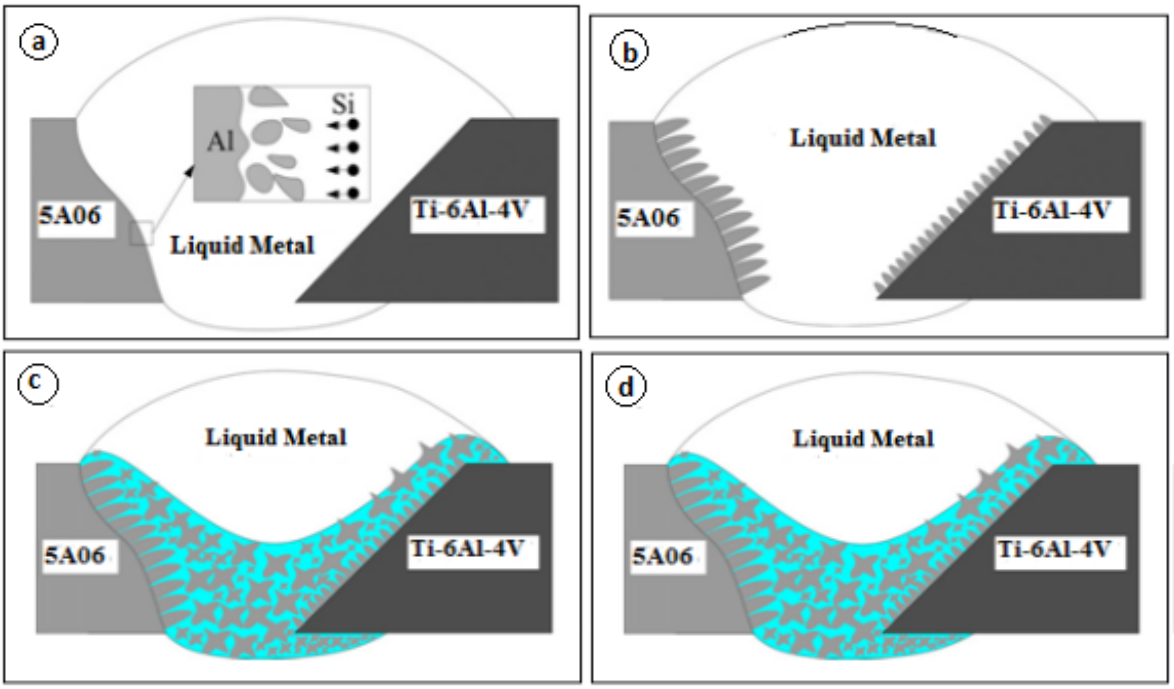

Fig. 15 Crystallization behavior of fusion welding joint, (a) Formation of weld pool and diffusion of element Si, (b) Formation of CCZ, (c) Solidification of the seam and (d) Formation of the joint

The fusion welding zones as fusion line, CCZ and ECZ have been discussed by using 5A06 and Ti6Al4V combination [44]. The microstructures of welding joint consist of Al grains and ternary near eutectic structure including Al, Si and Mg_2Si. Fusion line with fine hypoeutectic microstructure is formed by diffusion of element Si from weld pool to semi molten zone at solid and liquid interface. The columnar crystal formed due to obvious directionality of heat conduction is shown in Figs. 15 (a)-(d). Equiaxed crystals are formed in the weld pool due to the stir by filler wire and high degree of super cooling. The microstructures of brazing zone are orderly from Ti alloy to the seam consists of Ti nano size granular $Ti_7Al_5Si_{12}$ and serration shaped $TiAl_3$. Apparent stacking fault structure of IMC $TiAl_3$ is found. During the interfacial reaction at solid and liquid interface the formation of $Ti_7Al_5Si_{12}$ depended on the dissolution of Ti alloy and the segregation of Si atoms and IM phase $TiAl_3$ is formed by the crystallization. Growth of brittle reaction layer could be suppressed because dissolution of Ti alloy is weakened by formation of ternary compound $Ti_7Al_5Si_{12}$.

III. Conclusion and Future Scope

The outcome of the literature review, research and developments in Ti/Al alloys welded by using LBW are as follows:

1. The detailed analysis of problems faced during welding of Ti/Al dissimilar metal combination has been discussed.
2. Analysis of Ti/Al weldment with respect to HAZ, IMC, FZ, fracture and weld metal of joint by metallurgical feature has been shared.
3. The paper provides a detailed literature review of dissimilar metal property variation across the Ti/Al alloys weldment.
4. The development of LBW is the experimental stage for the past decade using various metal combinations.
5. The applicability of laser welding process for industrial purposes is constrained by several key technical issues that need to be further investigated.
6. Many researches mainly focused on laser welding of conventional materials. Ti/Al dissimilar combinations are worked by few researches.
7. More studies on properties of Ti/Al dissimilar metal need to be addressed to gain a better understanding of the laser welding process.

References

[1] Michael. K, Florian. W, Frank. V, 2005, 'Laser processing of Al–Ti-tailored blanks'. Opt. Laser Eng. 43, 1021–1035.
[2] Bondar. A.A, Witusiewicz. V.T, Hecht. U, Remez. M.V, Voblikov. V.M, Tsyganenko. N.I, Yevich. Y.I, Podrezov. Y.M, Velikanova. T.Y, 2011, 'Structure and Properties of Ti–Al Alloys Doped Wit-*/h Niobium and Tantalum'. Powder Metall. Metal Ceram, 50, 7–8.
[3] Luo. J.G, Acoff. V.L, 2000, 'Interfacial Reactions of Ti and Al during Diffusion Welding'. Suppl. Weld. J, 79, 239s–243s.
[4] Dressler. U, Biallas. G, Mercado. U.A, 2009, 'Friction stir welding of Ti alloy TiAl6V4 to aluminium alloy AA2024-T3'. Mater. Sci. Eng. A, 526, 113–117.
[5] Chen. Y, Liu. C, Liu. L, 2011, 'Study on the Joining of Ti and Al Dissimilar Alloys by Friction Stir Welding'. Open Mater. Sci. J. 5, 256–261.

[6] G. Casalino, 2017, 'Advances in Welding Metal Alloys, Dissimilar Metals and Additively Manufactured Parts'. Metals, 7, Issue 2, 1 February, Article number 32

[7] M. Mazar Atabaki, N. Yazdian, R. Kovacevic, 2016, 'Partial penetration laser-based welding of aluminum alloy (AA 5083-H32)'. Optik 127, 6782–6804.

[8] Atabaki, M.M., Yazdian, N., Ma, J., Kovacevic, R 2016, 'High power laser welding of thick steel plates in a horizontal butt joint configuration'. Optics and Laser Technology, 83, 1-12.

[9] L. Quintino, A. Costa, R. Miranda, D. Yapp, V. Kumar, C. J. Kong, 2007, 'Welding with high power fiber lasers–a preliminary study'. Materials and design, 28, 1231-1237.

[10] Chen. Y, Chen. S, Li. L, 2010, 'Influence of interfacial reaction layer morphologies on crack initiation and propagation in Ti/Al joint by laser welding–brazing'. Mater. Des. 31, 227–233.

[11] Chen. S, Li. L, Chen. Y, Dai. J, Huang. J, 2011, 'Improving interfacial reaction nonhomogeneity during laser welding–brazing Al to Ti'. Mater. Des. 32, 4408–4416.

[12] Casalino. G, Mortello. M, Campanelli. S, 2015, 'Ytterbium fiber laser welding of Ti6Al4V alloy'. J. Manuf. Process. 20, 250–256.

[13] Lee, Su-Jin, Nakamura, Hiroshi, Kawahito, Yousuke, Katayama, Seiji 2013, 'Weldability of Ti and Al Dissimilar Metals Using Single-Mode Fiber Laser', Journal of Laser Micro Nano Engineering, vol. 8.2, pp. 149-154.

[14] Casalino. G, Mortello. M, 2016, 'Modeling and experimental analysis of fiber laser offset welding of Al-Ti butt joints'. Int. J. Adv. Manuf. Technol. 83, 89–98.

[15] Casalino. G, Mortello. M, Peyre. P, 2015, 'Yb-YAG laser offset welding of AA5754 and T40 butt joint'. J. Mater. Process. Technol. 223, 139–149.

[16] Leo. P, D'Ostuni. S, Casalino. G, 2018, 'Low temperature heat treatments of AA5754-Ti6Al4V dissimilar laser welds: Microstructure evolution and mechanical properties'. Opt. Laser Technol. 100, 109–118.

[17] Casalino. G, Guglielmi. P, Lorusso. V.D, Mortello. M, Peyre. P, Sorgente. D, 2017, 'Laser offset welding of AZ31B magnesium alloy to 316 stainless steel'. J. Mater. Process. Technol. 242, 49–59.

[18] Casalino. G, Leo. P, Mortello. M, Perulli. P, Varone. A, 2017, 'Effects of laser offset and hybrid welding on microstructure and IMC in Fe-Al dissimilar welding'. Metals. 7, 282.

[19] Wang. H, Feng. B, Song. G, Liu. L, 2018, 'Laser–arc hybrid welding of high-strength steel and aluminum alloy joints with brass filler'. Mater. Manuf. Processe. 33, 735–742.

[20] NI Jia-ming, LI Li-qun, CHEN Yan-bin, FENG Xiao-song, 2007, 'Characteristics of laser welding-brazing joint of Al/Ti dissimilar alloys', The Chinese Journal of Nonferrous Metals, Vol.17 No.4.

[21] Giuseppe Casalino, Sonia D'Ostuni, Pasquale Guglielmi, Paola Leo, Michelangelo Mortello, Gianfranco Palumbo, Antonio Piccininni, 2017, 'Mechanical and microstructure analysis of AA6061 and Ti6Al4V fiber laser butt weld', Optik, vol.148, pp. 151-156.

[22] Shuhai Chen, B, Liqun Lib, Yanbin Chenb & Jihua Huanga 2011, 'Joining mechanism of Ti/Al dissimilar alloys during laser welding-brazing process', Journal of Alloys and Compounds, vol. 509, Issue 3, 21, pp. 891-898.

[23] S. H. Chen, L Q. Li, Y B. Chen, 2008, 'Interfacial reaction mode and its influence on tensile strength in laser joining Al alloy to Ti alloy', Materials Science and Technology, mst8587.3d.

[24] Sujin Lee, Seiji Katayama & Jong-Do Kim 2014, 'Microstructural behaviour on weld fusion zone of Al-Ti and Ti-Al dissimilar lap welding using single-mode fiber laser', Journal of the Korean Society of Marine Engineering, vol. 38, no. 2 pp. 133-139.

[25] Xiongfeng Zhou, Jian Duan, Fan Zhang, Shunshun Zhong, 2019, 'The Study on Mechanical Strength of Titanium-Aluminum Dissimilar Butt Joints by Laser Welding-Brazing Process', Materials, 12, 712.

[26] Song. Z.H, Nakata. K, Wu. A, Liao. J.S, 2013, 'Interfacial microstructure and mechanical property of Ti6Al4V/A6061 dissimilar joint by direct laser brazing without filler metal and groove'. Mater. Sci. Eng. A, 560, 111–120.

[27] Vaidya. WV, Horstman. V, Ventzke. V, Petrovski. B, Koçak. M, Kocik. R, Tempus. G 2009, 'Structure-property investigations on a laser beam welded dissimilar joint of aluminium AA6056 and titanium Ti6Al4V for aeronautical applications. Part II: Resistance to fatigue crack propagation and fracture', Materials Science & engineering Technology, vol. 40, Issue 10, pp. 769-779.

[28] Tomashchuk. P, Sallamand. E, Cicala. P, Peyre. D, Grevey, 2014, 'Direct keyhole laser welding of aluminum alloy AA5754 to titanium alloy Ti6Al4V', Journal of Materials Processing Technology - Vol. 217, p.96–104.

[29] Shuhai Chen, Li-Qun LI, Yan-bin Chen, De-Jian LIU, 2010, 'Si diffusion behavior during laser welding-brazing of Al alloy and Ti alloy with Al-12Si filler wire', Transactions of Nonferrous Metals Society of China, vol. 20, Issue 1, pp. 64-70.

[30] Xin Xue, António Pereira, Gabriela Vincze, Xinyong Wu, Juan Liao, 2019, 'Interfacial Characteristics of Dissimilar Ti6Al4V/AA6060 Lap Joint by Pulsed Nd:YAG Laser Welding', Metals, 9, 71.

[31] Marina Bulanova, Ludmila Tretyachenko, Marina Golovkova, Konstantin Meleshevich 2004, 'Phase equilibria in the α-Ti-Al-Si region of the Ti-Si-Al system', Journal of Phase Equilibria and Diffusion', vol. 25, Issue. 3, pp. 209-229.

[32] Ming Gao, Cong Chen, Yunze Gu and Xiaoyan Zeng, 2014, 'Microstructure and Tensile Behavior of Laser Arc Hybrid Welded Dissimilar Al and Ti Alloys', Materials, 7, 1590-1602.

[33] Lv. S.X, Jing. X.J, Huang. Y.X, Xu. Y.Q, 2012, 'Investigation on TIG arc welding-brazing of Ti/Al dissimilar alloys with Al based fillers. Sci. Technol. Weld. Join. 17, 519–524.

[34] Da Quan Zhang, Jin Li, Hyung Goun Joo, Kang Yong Lee, 2009, 'Corrosion properties of Nd:YAG laser–GMA hybrid welded AA6061 Al alloy and its microstructure', Corrosion science, vol.51, pp.1399-1404.

[35] Patrice Peyrea, Laurent Berthea, Morgan Dala, Sébastien Pouzeta, Pierre Sallamandb, Iryna Tomashchuk, 2014, 'Generation and characterization of T40/A5754 interfaces with lasers', Journal of Materials Processing Technology 214, 1946–1953.

[36] Lee, Sujin, Nakamura, Hiroshi, Kawahito Yousuke, Katayama Seji, 2013, 'Microstructural Characteristics and Mechanical Properties of Single-Mode Fiber Laser Lap-Welded Joint in Ti and Al Dissimilar Metals', Transactions of JWRI, vol. 42, no. 1, pp. 17-21.

[37] Giuseppe Casalino, Sonia D'Ostuni, Pasquale Guglielmi, Paola Leo, Gianfranco Palumbo, Antonio Piccininni, 2018, 'Off-Set and Focus Effects on Grade 5 Titanium to 6061 Aluminum Alloy Fiber Laser Weld', Materials, 11, 2337.

[38] Shant Prakash Gupta 2002, 'Intermetallic compounds in diffusion couples of Ti with an Al-Si eutectic alloy', Materials Characterization, vol.49, Issue 4, pp. 321-330.

[39] Yanbin Chen, Shuhai Chen, Liqun Li, 2008, 'Effects of heat input on microstructure and mechanical property of Al/Ti joints by rectangular spot laser welding-brazing method', Int J Adv Manuf Technol, DOI 10.1007/s00170-008-1837-2.

[40] Cabibbo, M, Marrone, S, Quadrini, E, 2005, 'Mechanical and microstructural characteristics of laser welded titanium–aluminium joints', Weld Int, vol. 19, pp. 125 -129.

[41] Zhihua Song, Kazuhiro Nakata, Aiping Wub, Jinsun Liao, 2012, 'Interfacial microstructure and mechanical property of Ti6Al4V/A6061 dissimilar joint by direct laser brazing without filler metal and groove', Materials Science & Engineering A 560, 111–120.

[42] Tomashchuk. P, Sallamand. A, Méasson. E, Cicala. M, 2017, 'Aluminum to titanium laser welding-brazing in V-shaped grooveI'. Journal of Materials Processing Technology, 245, pp.24-36.

[43] Mohammed Naeem, "Microwelding performance comparison between a low power (125W) pulase ND:YAG laser and a low power (100- 200W) single mode fiber laser", (2008). Proceedings of the 3rd Pacific International Conference on Application of Lasers and Optics.

[44] Shuhai Chen, Liqun Li, Yanbin Chen, and Jihua Huang, "Joining mechanism of Ti/Al dissimilar alloys during laser welding-brazing process", (2011). Journal of Alloys and Compounds 509, 891–898.